



Page No.

1. Yu. O. Starovoit, V.G. Kunakov and P. N. Martysevich  
- *About Dynamical Calibration of Microbarometers*
12. M. A. Zumberge - *Postdoctoral Scientist as Green Scholar at IGPP-SIO-UCSD*

---

## About Dynamical Calibration of Microbarometers

Yu. O. Starovoit, V.G. Kunakov and P. N. Martysevich

### Abstract

*One of the IMS technical specifications for infrasound stations is that the frequency response of a microbarometer should be known within the 5% accuracy. Meeting this specification needs precise methods of dynamical calibration within the frequency pass band of the sensor. One of the general and well-known techniques of dynamical calibration of a microbarometer is to use known pressure changes simulated by volume changes within a special chamber attached to the microbarometer. However, the simulation of pressure oscillations using volume changes of the calibration chamber requires precise theoretical considerations, in light of the required accuracy of the calibration.*

*In this paper we provide an insight on the whole thermodynamic process inside the calibration volume and discuss the potential impact on the accuracy of calibration if some details of the thermodynamic process are neglected.*

**Key words:** Dynamical calibration, isothermal branch, adiabatic branch.

---

### InfraMatics Editorial Board

Michael Hedlin (*Chief Editor*): [hedlin@ucsd.edu](mailto:hedlin@ucsd.edu)  
Hank Bass (*East North America*): [pabass@olemiss.edu](mailto:pabass@olemiss.edu)  
David Brown (*Australia/southern oceanic islands*): [djb@rses.anu.edu.au](mailto:djb@rses.anu.edu.au)  
Xiaofeng Chen (*SE Asia*): [xiaofeng.chen@263.net](mailto:xiaofeng.chen@263.net)  
Paola Campus (*CTBTO/West Europe*): [paola.campus@ctbto.org](mailto:paola.campus@ctbto.org)  
Milton Garcés (*West North America/South America*): [milton@isla.hawaii.edu](mailto:milton@isla.hawaii.edu)  
Sergey Kulichkov (*Eastern Europe, West Asia*): [snk@omega.ifaran.ru](mailto:snk@omega.ifaran.ru)  
Manohar Lal (*S Asia/Africa*): [manoharlal\\_99@yahoo.com](mailto:manoharlal_99@yahoo.com)

---

InfraMatics is an informal series to make available in a timely fashion information about the science of infrasound that any of us might develop. It is provided via our organization's website [www.inframatics.org](http://www.inframatics.org). We expect contributions to InfraMatics to be short and cover only one distinct subject. Figures can be hand-drawn. Lengthy formulae can be stated without derivation. Contributions should be sent to any member of the editorial board by electronic mail. We will assemble all contributions received during a quarter into a single newsletter. The information may be duplicated in the website. We expect that all of us will publish papers that use the material we have previously forwarded to InfraMatics. Everyone is encouraged to do so. To avoid having the material used by someone else in earlier publication, we require that permission to use the material contained in the InfraMatics newsletter by anyone other than the author requires permission by the InfraMatics editorial board. For the time being, Michael Hedlin will act on behalf of the editorial board in such matters.

### 1. Introduction

This paper describes the method of dynamical calibration of a microbarometer using the chamber with variable volume. The physics of this method is based on the thermodynamic process occurring inside the closed volume and on the corresponding relationships between pressure, volume and temperature changes caused by the movement of the piston attached to the inlet of the chamber. The method has been already used in several applications [1, 2], however we consider essential to analyze its physical details.

### 2. Methodology

The goal of the calibration is to measure, with a fixed accuracy, the frequency response of a microbarometer to the known pressure changes. It is assumed that a microbarometer under calibration is connected to a data acquisition system with a defined sensitivity lying within the passband of interest.

As depicted in Figure 1, the calibration device is usually constituted by a calibration volume (chamber) **1** associated to a moving “piston”, which provides variations of the volume  $V$ . Pressure oscillations, associated with these volume changes are transmitted via a short pipe to the input of the microbarometer. A schematic diagram of the calibrator is shown in Figure 1.

Let us assume that sinusoidal pressure variations  $\Delta P$  have been induced by volume changes  $\Delta V$ . Since the process within the volume is non-isothermal, temperature oscillations  $\Delta T$  should be observed inside the chamber as well.

The process inside the calibration volume can be described as the system of three equations [3]:

$$\begin{aligned}
 PV &= RT \text{ or } R\Delta T = P\Delta V + V\Delta P \\
 C_v\Delta T &= -P\Delta V + \Delta Q \\
 -\frac{d(\Delta Q)}{dt} &= \beta\Delta T
 \end{aligned}
 \tag{1}$$

where the first equation is the ideal-gas equation, the second equation represents the 1<sup>st</sup> law of thermodynamics and the third one describes the heat exchange between the inner volume of the chamber and the external environment. In addition:

- $R$  is the gas constant
- $P$  is the air pressure inside the chamber
- $Q$  is the heat flow through the chamber walls
- $C_v$  is the thermal capacity under the constant volume
- $\beta$  is the heat exchange coefficient between the air inside the chamber and the external environment

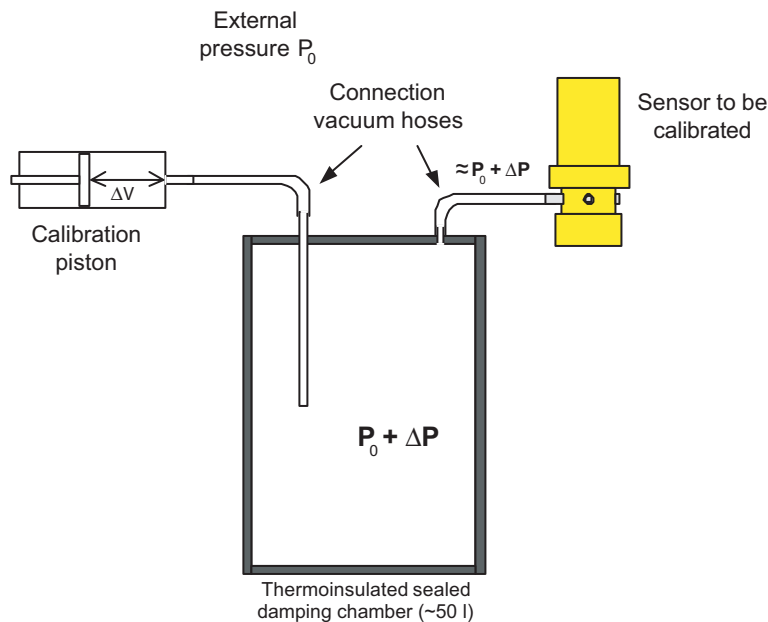


**Figure 1.** The block - diagram of the calibration process.

Assuming  $\Delta V = \Delta V_0 e^{i\omega t}$ , where  $\omega$  is the angular frequency associated to the sinusoidal variations of the volume oscillations, and  $\Delta V_0$  is the amplitude of volume changes, it is possible to obtain the solution of the system (1) above in the following form:

$$\Delta P = \frac{P}{V} \cdot \gamma \cdot \frac{(p + \beta / C_p)}{(p + \beta / C_v)} \Delta V \quad (2)$$

where  $\gamma = \frac{C_p}{C_v} = 1.4$  is the adiabatic coefficient and  $p = i\omega$  is a complex angular frequency. Equation (2) thus describes the transfer function of pressure changes inside the volume  $V$  caused by small volume oscillations  $\Delta V$ .

The corresponding temperature changes inside the volume could be written as follows:

$$\Delta T = -\frac{P_0}{C_v} \frac{1}{(p + \beta / C_v)} \cdot \Delta V \quad (3)$$

Both equations (2) and (3) show that oscillations of internal pressure and temperature have a phase shift relative to volume changes and, depending from the angular frequency  $\omega$ , have induced variations of different amplitude.

### 3. Design of the Calibration Chamber

The calibration chamber should be designed in such a way that the pressure oscillations, caused by the volume changes, should have the same and finite amplitude within the passband of interest, defined by the nominal frequency response of a microbarometer being calibrated. The transfer function, described by equation (2), gives the information about the difference in pressure oscillations amplitudes depending on the frequency. For design purposes, one needs to estimate the values of two cut-off frequencies

$\omega_1 = \frac{\beta}{C_p}$  and  $\omega_2 = \frac{\beta}{C_v}$ , which are responsible for the shape of the transfer function.

The main difficulty comes from the estimation of  $\beta$ . This coefficient describes the rate of the heat exchange between the air inside and outside of the chamber or, in other words, how close is the thermodynamic process inside of the chamber to its adiabatic or isothermal branch. The coefficient  $\beta$  could be written in the following form [3]

$$\beta = \frac{\lambda \cdot S}{h} \quad (4)$$

where  $\lambda$  is the thermal conductivity of the chamber walls material,  $S$  is the surface area of the chamber and  $h$  is the wall thickness. If we consider the cut-off frequency  $\omega_p$ , we can re-write its expression as:

$$\omega_1 = \frac{\beta}{C_p} = \frac{\lambda \cdot S}{h \cdot \rho V c_p} \quad (5)$$

where  $C_p = \rho V c_p$ ;  $c_p$  is the specific heat,  $\rho$  is the air density and  $V$  is the chamber volume.

It can be shown easily that the ratio  $S/V$  for a cubic shape of the calibration chamber is equal to  $6/l_0$ , where  $l_0$  is the edge of the cube. The cut-off frequency in (5) thus equals:

$$\omega_1 = \frac{6 \cdot \lambda}{h \cdot \rho c_p \cdot l_0} \quad (6)$$

and, similarly:

$$\omega_2 = \frac{6 \cdot 1.4 \cdot \lambda}{h \cdot \rho c_p \cdot l_0} = \frac{8.4 \cdot \lambda}{h \cdot \rho c_p \cdot l_0} \quad (7)$$

Formulas (6) and (7) allow the estimation of both cut-off frequencies in (2) and, therefore, permit the calculation of simulated pressure oscillations inside of the chamber caused by small volume changes induced by the piston. It is important to note that values of  $\omega_1$  and  $\omega_2$  depend not only on the thickness of the chamber walls and the type of material the chamber is made from, but also on the size of the chamber.

Assuming, for instance, that the calibration chamber is made of steel with a thickness of the walls of about  $h = 2 \cdot 10^{-3} \text{ m}$  and  $l_0 = 2 \cdot 10^{-1} \text{ m}$ , one can get an estimate of  $\omega_1$  and  $\omega_2$ :

$$\omega_1 = 198 \cdot 10^2 \frac{\text{rad}}{\text{sec}} \quad \text{and}$$

$$\omega_2 = 2.78 \cdot 10^2 \frac{\text{rad}}{\text{sec}}.$$

The shape of this normalized transfer function is shown by the black curve in Figure 2.

The thermal insulation of the chamber walls with materials having lower thermal conductivity dramatically changes the values of the cut-off frequencies. In this case the process inside of the chamber is more close to be adiabatic and using, for example  $\sim 5 \text{ mm}$  of cork or cotton insulation for the same size of the calibration chamber, we get the following values of  $\omega_1$  and  $\omega_2$

$$\omega_1 = 1.5 \cdot 10^{-1} \frac{\text{rad}}{\text{sec}} \quad \text{and}$$

$$\omega_2 = 2.1 \cdot 10^{-1} \frac{\text{rad}}{\text{sec}}.$$

The transfer function for this case is shown by the red curve in Figure 2.

Both red and black curves in Figure 2 are not flat in the passband of interest from 0.01 to 20

Hz. It means that equal volume oscillations injected by the piston cause variable pressure changes depending on the frequency of oscillations. This result is far from being ideal. However, a simple increase of the thickness of insulation material up to 20 mm and a slight increase of the volume of the calibration chamber up to  $\sim 75$  liters, will dramatically improve the situation and will lead to the shape of the response as it is shown by pink dots in Figure 2. Yet, as it can be seen from Figure 2, the transfer function shown with the pink dots is still not completely flat in the passband of interest and is attenuated by about 10% at the corner frequency of 0.01 Hz. This fact needs to be taken into account in the calibration process.

At a first glance, the use of the isothermal branch of the transfer function (lower part of the black curve in Figure 2) could appear more attractive, since its shape is almost flat up to 8 Hz. However, the quick heat exchange between the internal volume and the external ambient ( $\lambda$  is high in this case) might cause undesirable results, like abrupt external temperature changes during the calibration process reflecting into the values of induced pressure oscillations and thus introducing significant errors in the calibration process.

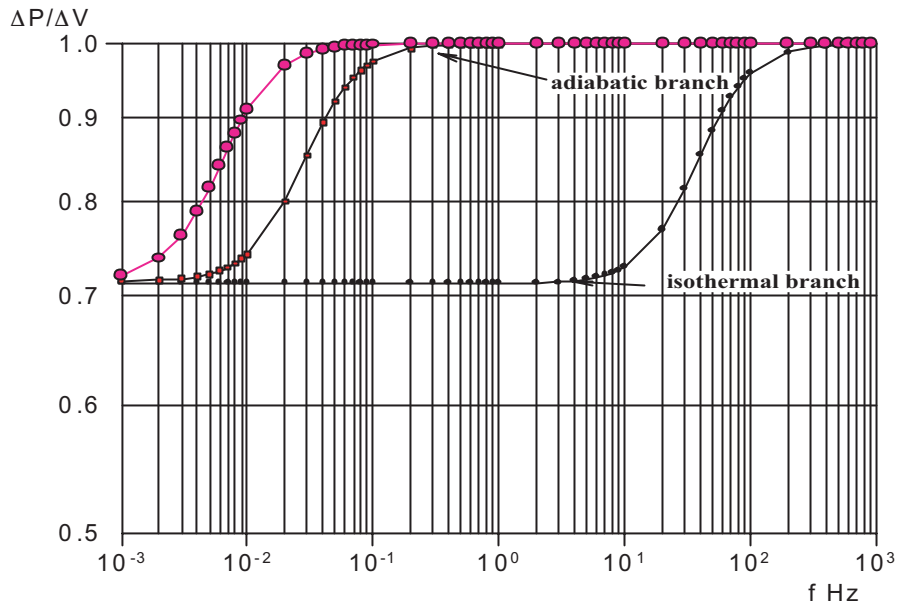


**Figure 2.** Normalized transfer functions of internal pressure changes caused by volume oscillations. The details of the curves are explained in the text.

#### 4. Modeling of the Calibration Process

The considerations above allow an easy simulation of the calibration process and permit a comparison with the result of the field experiment in one of the IMS infrasound station.

The prototype of the calibration device has been designed in the Institute of Geophysical Research of the Republic of Kazakhstan. The calibration chamber was made of steel with the wall thickness of 2 mm and had a cubic volume of approximately 0.05m<sup>3</sup>. The thermal insulation of the calibration volume has been achieved using two layers of woolen material glued to the walls. For the purpose of additional thermal insulation this volume has been placed inside a special wooden box, to protect the calibration volume against direct contact with the surrounding atmosphere.

The syringe, connected to the calibration volume by means of a thick-wall short rubber pipe, has been used for introducing a known variation of the volume of air (~10-15 cm<sup>3</sup>) and therefore, for simulating the pressure changes as described by equation (2). The movement of the syringe's piston should be done as fast as possible in order to inject the volume change as a step function input signal. The syringe used as prototype has made it possible to inject 10 cm<sup>3</sup> of air within ~10

milliseconds. Such short ramping time of the input signal assures flatness of the input spectrum within the passband of interest. Therefore, further estimates of the sensor frequency response have been done using spectral analysis of the transient response of the microbarometer to the step function input.

The microbarometer MB2000 (DASE, France) has been calibrated with such a device. This sensor has two outputs for pressure changes. One of them has the flat frequency response from 0.01Hz up to 8Hz with a sensitivity of 20mV/Pa, which is described by one zero and four poles as explained in [4] (from now onward it will be called the "filtered output"). The second output has the flat response up to DC with sensitivity of 1 mV/Pa and the high frequency cut-off equals to 8 Hz as well. Actually, the high frequency cut-off is defined by the design of the data logger FIR filters and depends on the digitizer sampling rate. Since for CTBTO purposes a 20 Hz sampling rate is usually used for infrasound data, the 8 Hz has been specified as the high frequency cut-off.

The experimental transient responses of the MB2000 to the step function are shown in Figure 3 and Figure 4 for filtered and DC outputs respectively. The calibration of the microbarometer has been carried out at IS31,

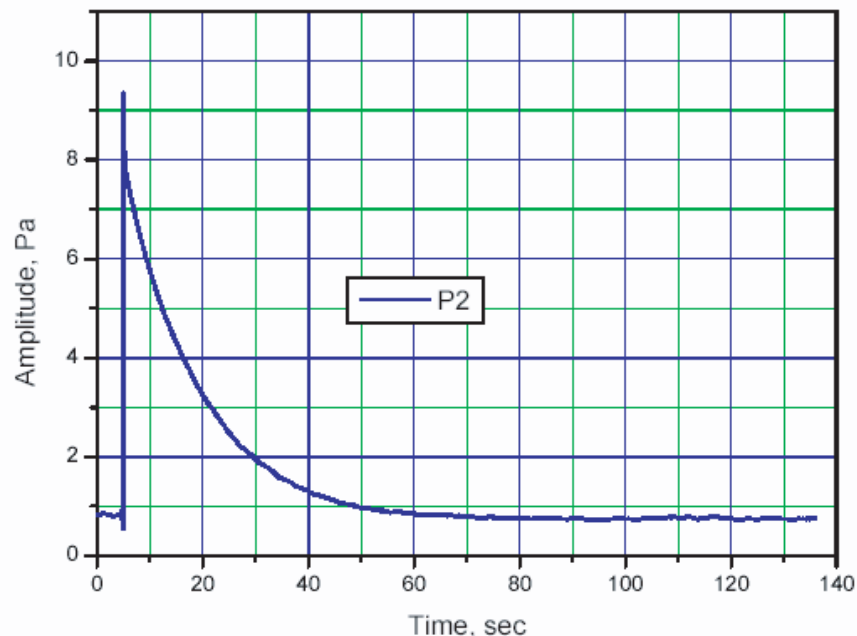


**Figure 3.** Transient experimental response of the filtered channel of MB2000 on a step function at IS31Aktyubinsk, Kazakhstan.

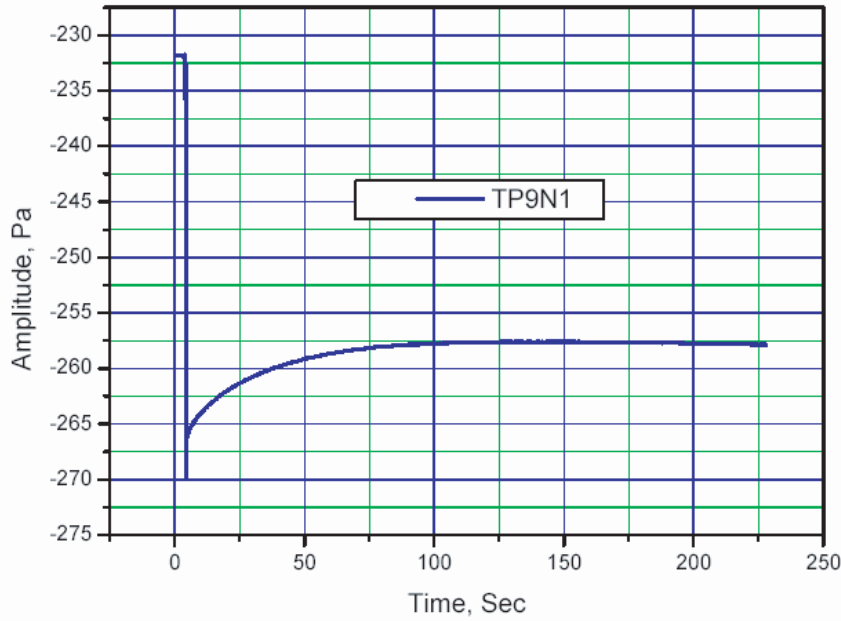


**Figure 4.** Transient experimental response of the DC channel of MB2000 on a step function at IS31 Aktyubinsk, Kazakhstan.

Aktyubinsk, Kazakhstan during Summer 2004. Significantly different shapes of the step response can be observed due to the different shape of channel’s transfer function.

Now let us compare the results of the field calibration with the nominal response of the microbarometer, taking into consideration the thermodynamic process in the calibration as described above by formula (2).

In accordance with (2) the overall channel response to the simulated step function describing the volume change could be expressed as follows

$$H_n(p) = H_a(p) \cdot \left[ -\frac{P}{V} \cdot \gamma \cdot \frac{(p + \beta / C_p)}{(p + \beta / C_v)} \right] \quad (8)$$

where

$$H_a(p)$$

is the actual or measured response of the channel based on the spectral transformation of the transient response function;

$H_n(p)$  is the nominal channel response as specified in the microbarometer documentation [4]. The term in square brackets corresponds to the distortion of the nominal response caused by the thermodynamic process inside the calibrator’s chamber as outlined in Section 2. From equation (8) it becomes clear that the response  $H_a(p)$  and  $H_n(p)$  will coincide only if the calibration volume will be designed in a such way that the second term in the product (8) will be negligible within the passband of interest for the MB2000. In other words the corner frequencies  $\omega_{1,2}$  should be placed well outside the microbarometer passband.

Poles and zeroes for  $H_n(p)$  of the MB2000 are given in the Table 1.

**Table 1. Poles and Zeroes of MB2000**

#	Poles		Zeroes	
	Re	Im	Re	Im
1	-1.777E+02	-1.777E+02	0.0	0.0
2	-1.777E+02	+1.777E+02		
3	-6.280E-02	0.000E+00		
4	-2.0734E+02	0.000E+00		

As it can be seen from the Table above, within the passband of interest for the MB2000, the shape of the frequency response is mainly determined by the third pole and by one zero. The complex conjugate poles  $-1.77E+02 \pm i1.777E+02$  and the pole  $-2.0434E+02$  are mainly responsible for the shaping of the response in the high-frequency domain when the sensor is being used with digitizer's sampling rate higher than 20 Hz. This simplification allows the representation of equation (4) in the form

$$H_a(p) = \frac{p}{p + \Omega_3} \cdot \left[ -\frac{P}{V} \cdot \gamma \cdot \frac{(p + \beta / C_p)}{(p + \beta / C_v)} \right] \quad (9)$$

where  $\Omega_3$  is the third pole in Table 1, which is equal to 6.28E-02.

Since  $H_a(p)$  in equation (9) takes the form of a product of two polynomial fractions in  $p$ , it is obvious that the simulation can be approximated by a cascade of two recursion filters in the time domain [5]. The transition from the  $p$  - plane of the continuous system to the  $z$  - plane of a sampled-data, with sampling interval  $\Delta t$  can be designed with the standard  $z$ -transform or the bilinear  $z$ -transformation [6]. This filter can be designed by well-known substitution [6]

$$p = \frac{2}{\Delta t} \cdot \frac{1 - z^{-1}}{1 + z^{-1}} \quad (10)$$

which defines the bilinear transformation where  $z^{-n}$  is regarded as a time shift operator. The index  $n$  indicates how many integer multiples of the sampling interval is involved in the time shift, with the sign of the index denoting whether it is a forward (plus sign) or backward (minus sign) shift. For example:  $z^{-n} x(t) = x(t - n\Delta t)$ .

The corner frequencies  $\omega_i$  of the analogous system (9) are converted to the corresponding digital values  $\omega'_i$  in accordance with

$$\omega'_i = \tan \left( \frac{\omega_i \cdot \Delta t}{2} \right) \quad (11)$$

Inserting equation (10) into (9) and substituting  $\omega_{1,2}$  and  $\Omega_3$  in accordance with (11) the  $z$ -transform  $H_a(z)$  of  $H_a(p)$  becomes

$$H_a(z) = \frac{Y(z)}{X(z)} = -\frac{P}{V} \cdot \gamma \cdot \frac{1 - z^{-1}}{1 + z^{-1}} \cdot \frac{1}{\left( \frac{1 - z^{-1}}{1 + z^{-1}} + \Omega'_3 \right)} \cdot \frac{\left( \frac{1 - z^{-1}}{1 + z^{-1}} + \omega'_1 \right)}{\left( \frac{1 - z^{-1}}{1 + z^{-1}} + \omega'_2 \right)} \quad (12)$$

where  $Y(z)$  is the output of the microbarometer and  $X(z)$  is the input volume changes simulated by the piston, connected to the calibration chamber.

Rearranging equation (12), the following recursion procedure can be obtained

$$Y(n) = a_1 Y(n-1) + a_2 Y(n-2) + a_3 X(n) + a_4 X(n-1) + a_5 X(n-2) \quad (13)$$

where  $a_i$  are the filter coefficients, which transform the input volume changes into the simulated microbarometer output. Omitting simple algebraic transformations, coefficients  $a_i$  could be expressed as follows

$$a_1 = \frac{2 - 1.57 \cdot 10^{-3} \tan \left( 1.5 \cdot 10^{-1} \cdot \frac{\lambda \gamma}{h \rho c_p l_0} \right)}{1.00157 \cdot \left[ 1 + \tan \left( 1.5 \cdot 10^{-1} \cdot \frac{\lambda \gamma}{h \rho c_p l_0} \right) \right]} \quad (14)$$

Denoting the denominator in (14) as

$$C_0 = 1.00157 \cdot \left[ 1 + \tan \left( 1.5 \cdot 10^{-1} \cdot \frac{\lambda \gamma}{h \rho c_p l_0} \right) \right]$$

the other coefficients can be rewritten as

$$a_2 = \frac{\tan\left(1.5 \cdot 10^{-1} \cdot \frac{\lambda}{h\rho c_p l_0}\right) - 1}{C_0} \quad (15)$$

$$a_3 = \frac{1 + \tan\left(1.5 \cdot 10^{-1} \cdot \frac{\lambda}{h\rho c_p l_0}\right)}{C_0} \quad (16)$$

$$a_4 = -\frac{2}{C_0} \quad (17)$$

$$a_5 = -a_2 = \frac{1 - \tan\left(1.5 \cdot 10^{-1} \cdot \frac{\lambda}{h\rho c_p l_0}\right)}{C_0} \quad (18)$$

Equation (13) allows an easy computation of the transient response of a microbarometer MB2000 to the volume changes expressed as a step function. Figure 5 and Figure 6 shows the response in the DC and filtered output, respectively. For the modeling purposes we assumed:

$$\omega_1 = 2\pi \cdot 0.005 \text{ Hz}$$

and

$$\omega_2 = 2\pi \cdot 0.007 \text{ Hz}$$

Figures 3, 5 and 4, 6 are very similar: this means that the procedure above used for simulating the channel response well reflects the behavior of the real MB2000 microbarometer under calibration. Note that by ignoring the transfer function by equation (2), the response of the microbarometer DC output should have had the shape as depicted in Figure 7.

The significant difference between the responses in Figures 4 (experimental), 6 (theoretical) and that one shown in Figure 7 is the clear demonstration that the effect of the thermodynamic process within the calibration volume should be taken into account. Therefore, the design of the calibration volume should aim to minimize the distortion caused by the thermodynamic process.

The easiest way to estimate the potential impact of the improper design (thermal insulation)

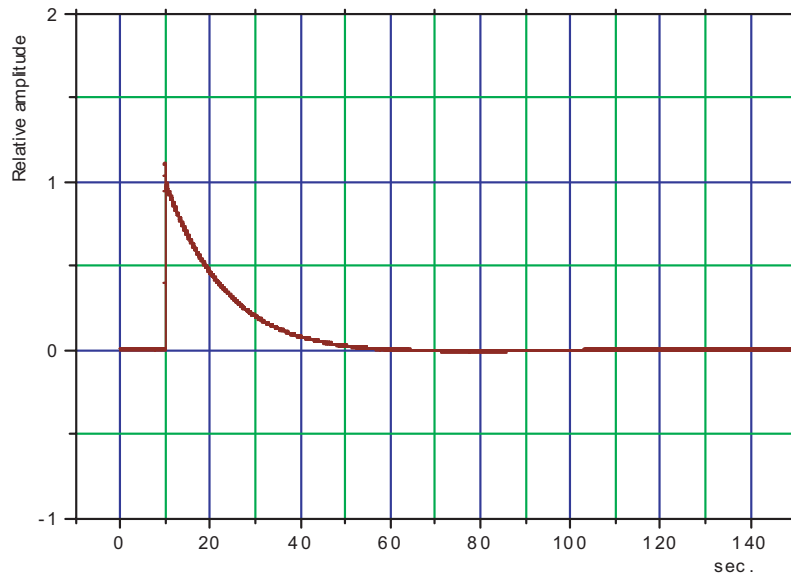


**Figure 5.** The calculated transient response of the filtered output of MB2000 to a step function.

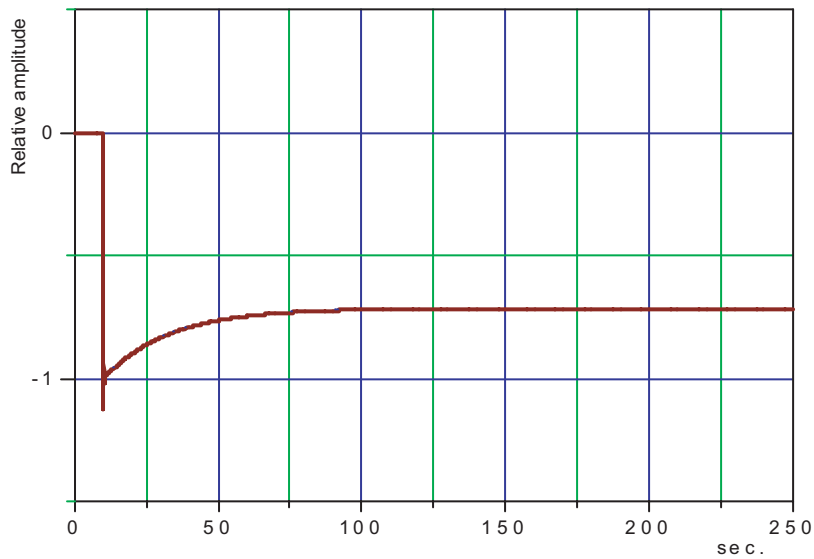


**Figure 6.** The calculated transient time response of the DC channel of MB2000 to a step function.

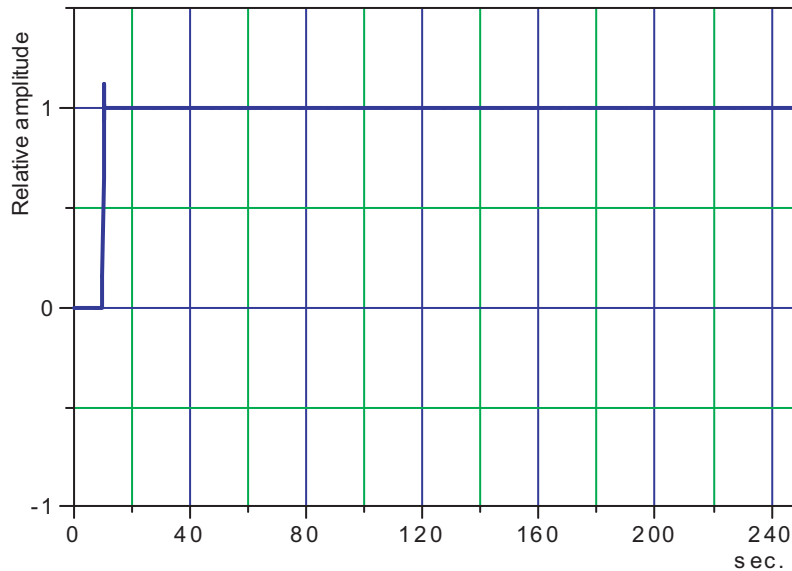


**Figure 7.** The calculated step-response of the pure DC channel without taking in to account the term described by equation (2).

of the calibration volume is to compute the filtered frequency response of the microbarometer based on the step response function. The conventional approach consists of calculating the spectral ratio between the output and the input signal as it is normally done for frequency responses. The two frequency responses in Figure 8 show the computations based on two different sets of values of  $\omega_1$  and  $\omega_2$ .

The computation of the blue curve has been based on the same frequencies used for the

transient response computation depicted in Figure 5. This curve corresponds well to the nominal response of the MB2000. The red curve has been obtained by using the improper design of the calibration volume, with  $\omega_1$  and  $\omega_2$ , reduced to 1/10 of the values used for the computation of the blue curve:

$$\omega_1 = 2\pi \cdot 0.05 \text{ Hz}$$

and

$$\omega_2 = 2\pi \cdot 0.07 \text{ Hz} .$$

The area where the two responses differ significantly is located within the blue ellipse. It can be seen that close to the channel cut-off frequency the error  $\epsilon$  is approximately 28%, which is well above required accuracy of calibration. Sharp spikes in the response curves for frequencies  $f > 1\text{Hz}$  is the evidence of the fact that input step function was not properly antialiased.

Figure 8 clearly demonstrates that the apparent distortion of the microbarometer frequency response shape could potentially happen not because of real changes of the sensor or of the data logger response, but due to the improper thermal insulation of the calibration volume, whenever the method of volume changes, described above, has been chosen for the verification of the channel frequency response.

### 5. Conclusion

The design of the calibration chamber for a dynamical calibration of microbarometer should take in to account the features of the

thermodynamic process inside the calibration volume. This process has been described in this paper by means of the transfer function of the induced pressure variations caused by small volume changes. It has been shown that the use of the adiabatic branch of this process requires taking into consideration the transfer function decay in the vicinity of the lower limit of the passband of interest.

Ignoring the thermodynamic details of the process may cause a distortion of the transfer function well above the required 5% accuracy of the calibration (see Figure 8).

A thermal insulation of the walls of the calibration volume or the placement of this volume inside of an additional insulation box appears to be a sufficient measure to assure that two critical corner frequencies  $\omega_1$  and  $\omega_2$  have the values well beyond the frequency passband of the sensor being calibrated.

The size of the calibration volume equal to  $\sim 75$  liters has appeared to be sufficient to assure lack of the frequency response distortion. This is

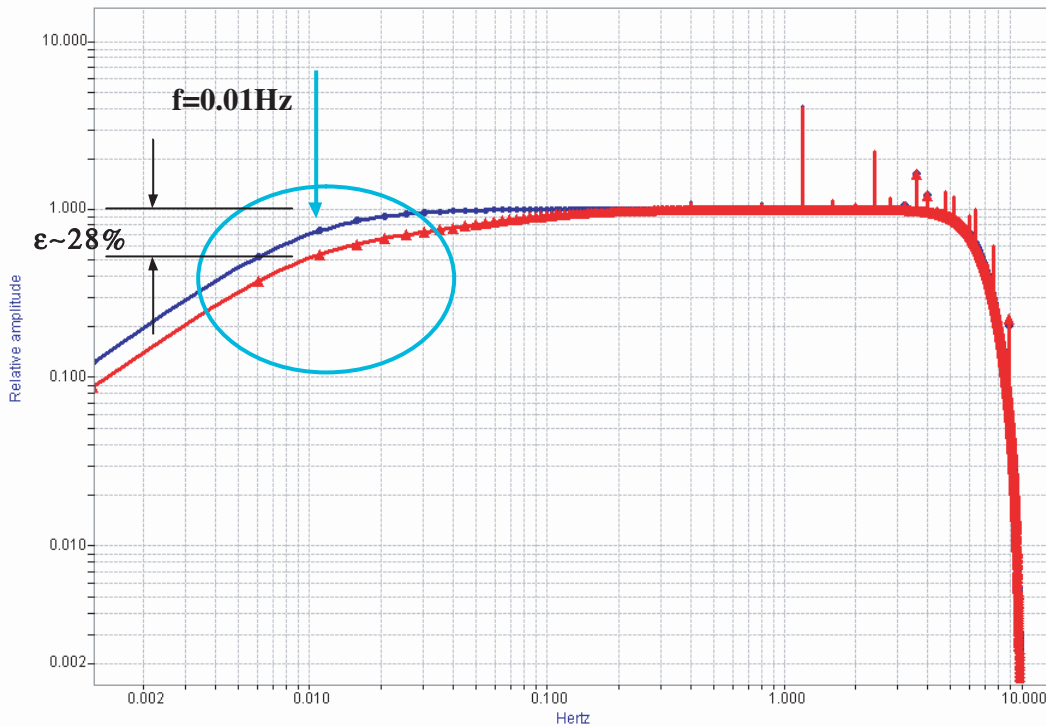


**Figure 8.** The normalized frequency response of MB2000 filtered channel based on the two sets of different values of  $\omega_1$  and  $\omega_2$ . Blue curve is for  $\omega_1=0.0314$  rad/sec and  $\omega_2=0.044$  rad/sec; the red curve is for  $\omega_1=0.314$  rad/sec and  $\omega_2=0.440$  rad/sec.

certainly true only under the condition of the proper thermal insulation of the calibration chamber, as it is explained above.

## 6. Acknowledgements

We would like to express our gratitude to station operator of IS31, Aktyubinsk in Kazakhstan for their logistics support during field calibration experiment in August 2004.

We thank Dr. Paola Campus (CTBTO/IMS) for thorough reading of our paper and many useful comments and suggestions.

## 7. References

1. *Kunakov, V., and P. Martysevich.* Dynamic calibration of an Infrasound Data Acquisition System (MB2000 microbarometer and Aubrac digitizer). Infrasound Technology Workshop, October 27 to 30, 2003, La Jolla, California, US. [http://12a.ucsd.edu/meeting/pdf/ITW\\_booklet.pdf](http://12a.ucsd.edu/meeting/pdf/ITW_booklet.pdf)
2. *Alcoverro, B.* Infrasound sensor dynamic calibration device. Infrasound Technology Workshop Kailua-Kona, Hawaii, 12-15 November, 2001. [http://www.isla.hawaii.edu/assets/downloads/meeting\\_abstracts.pdf](http://www.isla.hawaii.edu/assets/downloads/meeting_abstracts.pdf)
3. *Wark, Kenneth and Richards, Donald E.* Thermodynamics, 6th Ed., McGraw-Hill, 1999.
4. Technical Manual of microbarometer MB2000. Laboratoire de Gephysique, LDG France, December 1996.

5. *Beauchamp, K. G.* Signal processing. London: George Allen&Unwin LTD, 1973.

6. *Kaiser, J. F.* Design methods for sampled data filters. Proc.1<sup>st</sup> Annu. Allerton Conf. Circuit System Theory, pp.221-236. 1963.

## Contact the Authors:

Yu. O. Starovoit  
[yuri.starovoit@ctbto.org](mailto:yuri.starovoit@ctbto.org)

P. N. Martysevich  
[pavel.martysevich@ctbto.org](mailto:pavel.martysevich@ctbto.org)

International Monitoring System Division (IMS),  
Comprehensive Nuclear Test-ban-Treaty Organization (CTBTO),  
5, Wagramerstrasse , A-1400,  
Vienna  
Austria

V.G. Kunakov  
[vkunakov@kndc.kz](mailto:vkunakov@kndc.kz)

Institute of Geophysical Research, Republic of  
Kazakhstan  
4 Lizi Chaikinoy str.  
480020 Almaty  
Kazakhstan

## Postdoctoral Scientist as Green Scholar at IGPP-SIO-UCSD

M. A. Zumberge

The Institute of Geophysics and Planetary Physics (IGPP) at Scripps Institution of Oceanography (SIO) at the University of California San Diego (UCSD) has openings for one or more postdoctoral scientists as Green Scholars in the field of earth sciences. Joint funding from the Green Foundation for Earth Sciences and extramural sources associated with specific research projects are available to support postdoctoral positions. Emphasis is placed on candidates with a demonstrated ability to work with observational and/or modeling aspects of electromagnetism, geodesy, geomagnetism, glaciology, information technology for sensor networks, infrasound, ocean observatories, remote sensing, scientific visualization, seismology, and tectonics. Applicants should identify which of these fields are of primary interest.

The positions are available for one year and are renewable subject to satisfactory performance and availability of funds. Salary will be determined by UCSD, commensurate with qualifications and experience and based on UC salary scales. Applicants should send a Resume with the names of at least two references, immigration status, and the expected Ph.D. completion date to:

Green Scholar Selection Committee c/o Michell Parks, Institute of Geophysics and Planetary Physics (IGPP), MC 0225, Scripps Institution of Oceanography, University of California, San Diego, 9500 Gilman Drive, La Jolla, CA 92093-0225.

Applications will be accepted until the positions are filled. The University of California is an equal opportunity / affirmative action employer with a strong institutional commitment to the achievement of diversity.

M. A. Zumberge  
[mzumberge@ucsd.edu](mailto:mzumberge@ucsd.edu)  
Mail Code 0225  
IGPP-SIO-UCSD  
La Jolla, CA 92093-0225  
Tel: 858-534-3533



IGPP and Scripps Crossing at SIO.